Original Research Article

Effect of silica nanoparticles modified with different concentrations of stearic acid on microstructure, mechanical & electrical properties of RTV-2 silicone rubber nanocomposite

Leila Sohrabi-Kashani[a,b] , Ashkan Zolriasatein[a]* , Bijan Eftekhari Yekta[b]

a Non-metallic Materials Research Group, Niroo Research Institute, Tehran, Iran

b School of Metallurgy and Materials Engineering, Iran University of Science and Technology, Tehran, Iran

ARTICLE INFORMATION

ABSTRACT

One of the main challenges in preparing ceramic-reinforced polymer nanocomposites is the agglomeration of nanoparticles. This problem has been solved by surface modification of nanoparticles. In this study, silica nanoparticles were modified with low-cost and environmentally-friendly stearic acid instead of high-cost silanes or hazardous fluorinated hydrocarbons. RTV-2 silicone rubber/SiO_2 nanocomposite films containing 1wt% and 3wt% silica modified with stearic acid:silica ratios of 2:1 and 1:1 were prepared, and the effects of different concentrations of stearic acid and silica on microstructure, hydrophobicity, mechanical and electrical properties were investigated. The microstructure of the samples was studied by field emission scanning electron microscopy. Spray and contact angle tests were also done to study the hydrophobicity. Increased hydrophobicity was observed with the incorporation of modified silica into RTV-2. Results of mechanical properties tests revealed that increased stearic acid concentration caused a deterioration in mechanical properties. Among all the composite and pure samples, the sample containing 3wt% silica modified with a lower amount of stearic acid exhibited the highest hardness, elongation at break, and tensile modulus. Results of electrical tests indicated that all composite samples had lower dielectric constant and dielectric loss factor and higher surface resistance compared to the pure sample.

Corresponding author, email: azolriasatein@nri.ac.ir (A. Zolriasatein).

Graphical Abstract
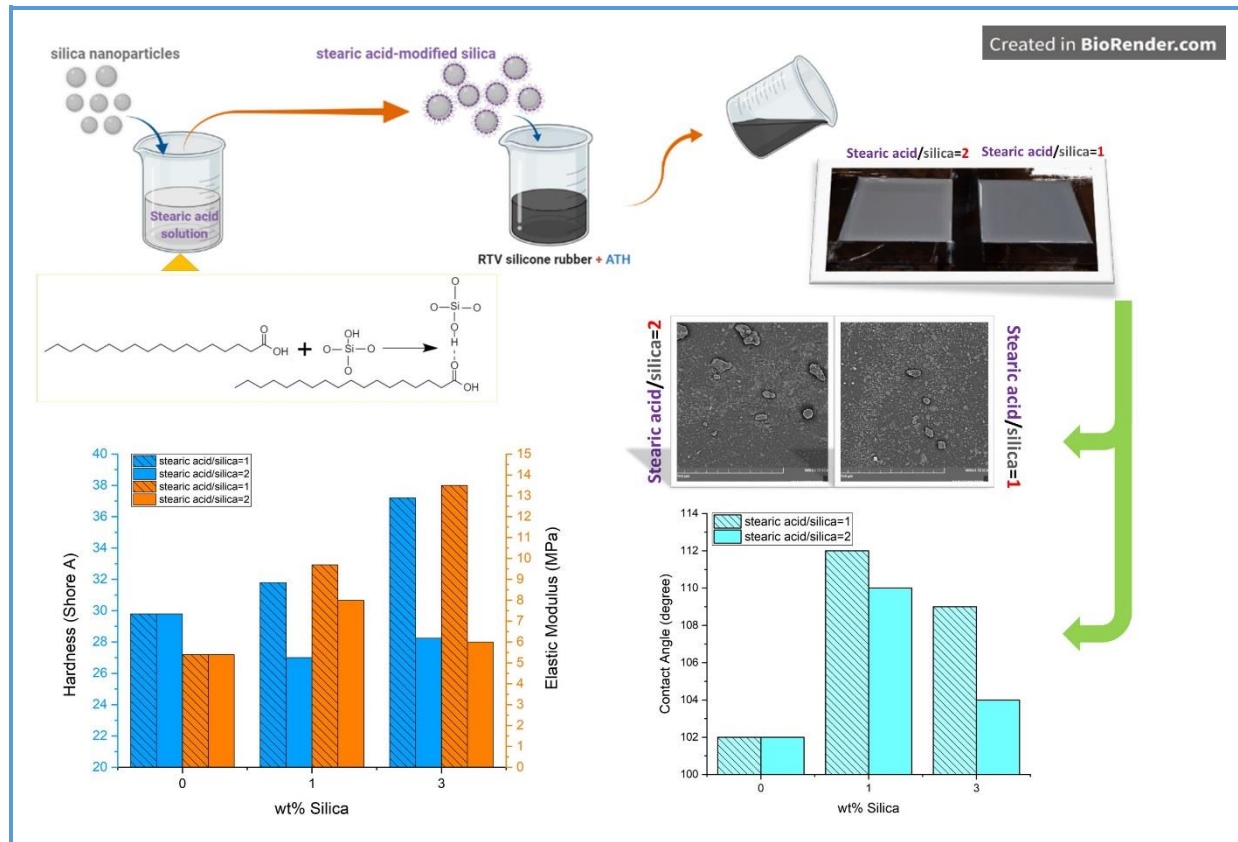
Introduction

Ceramic-reinforced polymer nanocomposites have improved mechanical, electrical [1-4], and superhydrophobic properties [5-10] compared to pure polymers. Coatings containing silica offer multiple benefits, including cost-effectiveness, enhanced hardness, and mechanical properties [11]. Researchers have successfully prepared superhydrophobic coatings with silica nanoparticles embedded into different polymers such as polystyrene-*b*-poly(ethylene-*co*-butylene)-*b*-polystyrene (SEBS) [5], polyurethane [6, 7, 12], acrylic polymer resin [13] and epoxy [14].

The polymer used in this research is a two-component room-temperature vulcanizing silicone rubber (RTV-2). RTV silicone rubber has been used as a coating for ceramic insulators [15, 16]. The deposition of contamination, particularly dust particles on the hydrophilic surface of ceramic outdoor insulators, and then moisture in the air cause electrical failure [17]. This will eventually lead to power outages and many problems. Hydrophobic nanocoatings can help to solve this problem [18]. Faezeh Farhang *et al.* [19] used aluminum trihydroxide (ATH) and unmodified microsilica fillers in RTV; however, no significant change in contact angle was noticed; SEM images demonstrated that silica particles had not been dispersed perfectly [19]. By using silica nanoparticles, M.Tariq Nazir *et al.* [20] improved the barrier resistance and hydrophobicity of RTV. Muhammad Amin *et al.* [21] reported that microsilica has no significant influence on the improvement of hydrophobic

behavior, and they concluded that the composite containing 10% micro-silica and 5% nano-silica had the best hydrophobic behavior and the least leakage current due to the strong interactions between silanol groups in nano-silica and silicone rubber network. Luiz H. Meyer *et al.* [22] used unmodified nano and micro silica as fillers in RTV, but when silica was added to the silicone rubber, the contact angle decreased. The mechanical properties of unmodified silica-reinforced composites were worse than those of the pure polymers due to the poor dispersion of fillers in the polymer matrix; these problems can be solved by surface modification of nanoparticles [23].

Silica nanoparticles are naturally hydrophilic and require suitable surface modification by chemical reaction or non-reactive modifiers to be incorporated into the polymer matrix [1, 24]. High-cost alkyl silane coupling agents have been widely applied as chemical surface modifiers [24]. Many researchers have used expensive hexamethyldisilazane (HMDS) for the surface modification of silica [25]. Fluorinated hydrocarbons are being used to turn the hydrophilic nature of silica into hydrophobic by replacing the hydroxyl group. However, modification with fluorinated hydrocarbons is expensive and hazardous to human health and the environment [11].

In this research, non-reacting and non-expensive stearic acid was used instead of expensive silane or fluorinated hydrocarbons. The nano-sized silica fillers modified with stearic acid were incorporated into polyether ether ketone (PEEK). The modified silica-filled PEEK nanocomposite showed a decrease in domain size and more uniform filler dispersion [24]. Poly(ethylene 2,6-naphthalate) (PEN) composites reinforced with stearic acid-modified silica exhibited increased elongation and decreased tensile modulus with increasing silica content [23]. Stearic acid-modified silica

nanoparticles were used to prepare silica-reinforced epoxy coatings, which showed considerably enhanced hardness and improved resistance to erosive wear [1]. Adsorbed stearic acid on the surface of silica can reduce the interaction between the silica nanoparticles and lower the size of agglomerates with increasing silica content [24]. These agglomerates can be broken down more easily [23].

It is essential to choose a suitable concentration of stearic acid to modify the surface of silica because if the proper concentration is not used, the properties of the composite will not only fail to improve but will also deteriorate. Therefore, silica nanoparticles were modified with two different ratios of stearic acid via a simple and cheap method. In addition to different concentrations of stearic acid, two concentrations of silica nanoparticles were also investigated. To the best of our knowledge, this is the first research that uses stearic acid as a surface modifier for preparing RTV-2/SiO$_2$ nanocomposite and investigates the effects of different silica concentrations with different modification ratios on microstructure, hydrophobicity, mechanical and electrical properties of RTV-2/SiO$_2$ nanocomposite. The composite preparation process is easy, including magnetic stirring and ultrasonication. This research study attempts to give insights into preparing a suitable coating for ceramic insulators.

Experimental

Materials

Ethyl acetate (99%), distilled water, granular type stearic acid (M_w =284.48, MP = 68–71°C, BP = 361 °C), two-component room temperature vulcanizing (RTV-2) silicone rubber (HY-215) from ShenZhen Hong Ye Jie Technology, aluminum trihydroxide (ATH) (Martinal ON-4608) from Martinswerk and

synthesized silica nanoparticles were used in this research. Silica nanoparticles had previously been synthesized through a precipitation method using hydrochloric acid, water glass, and CTAB as surfactant [26].
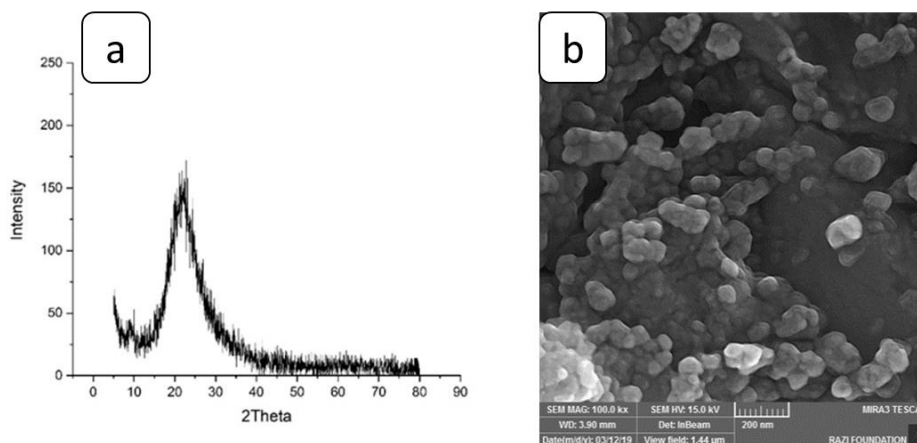
Figure 1 demonstrates the X-ray diffraction (XRD) pattern and field emission scanning electron microscopy (FE-SEM) images of silica nanoparticles used in this research. Figure 1(b) displays synthesized silica nanoparticles with a spherical morphology with an average particle size of about 30 nm.

Figure 1. a) XRD and b) FE-SEM image of silica nanoparticles used in this research [26]

Surface modification

Weight ratio of stearic acid:silica

First, 100 mL of ethyl acetate was poured into an Erlenmeyer flask, then 1.4 g of stearic acid was added. After stirring for 1 h, the solution became cloudy, and no stearic acid particles could be observed, indicating the complete dissolution of the stearic acid. In the next step, 0.7 g of silica nanoparticles were gradually added to the solution, followed by stirring for 1 h. The resulting mixture was filtered, and the modified particles were dried in the oven. Henceforth, nanoparticles modified with this ratio will be named se2.

Weight ratio of stearic acid:silica

0.5 g of stearic acid was added to 100 mL of ethyl acetate and stirred with a magnetic stirrer for 1 h. Then 0.5 g of silica nanoparticles were

gradually added to the solution and stirred for another hour. The resulting mixture was then passed through the filter paper, and the remaining particles were dried at 45 °C for 3 h. Henceforth, nanoparticles modified with this ratio will be named se1.

Composite preparation

Nanocomposite films containing different concentrations of silica modified with different amounts of stearic acid were prepared according to the formulations listed in Table 1. Toluene was poured into a glass beaker, then about half the amount of RTV was added, and the solution was stirred. Nanoparticles were gradually added, and the obtained mixture was homogenized by ultrasonic bath for 2 min. Next, the remaining amount of RTV was added under continuous stirring, then ATH was added. Once again, the resulting mixture was homogenized

in an ultrasonic bath for 3 min. In the last step, the hardener was added, and the mixture was stirred for 2–3 min. Sample rh with no silica content was also prepared, which will henceforth be known as the pure sample. The glass mold surface had been thoroughly cleaned using acetone and was perfectly level. Before pouring the composite onto the mold, a silicone separator was sprayed on, wax paper was placed on the mold, and the silicone was resprayed so that the composite films can be separated from the wax paper and the mold easily. After about 1 day at room temperature, the composite samples were ready for analysis. The samples are described in Table 2.

Table 1. Formulation of nanocomposite samples

Weight percent of silica in the composite	Silica(g)	ATH(g)	RTV(g)	Hardener(g) (0.1RTVwt)	Toluene(g) (0.4RTVwt)
1wt%: rhs1e1	0.113 (se1)	3.395 (30wt%)	7.8 (69wt%)	0.78	3.123
3wt%: rhs3e1	0.344 (se1)	3.44 (30wt%)	7.699 (67wt%)	0.769	3.07
1wt%: rhs1e2	0.226 (se2)	3.395 (30wt%)	7.8 (69wt%)	0.78	3.123
3wt%: rhs3e2	0.68 (se2)	3.44 (30wt%)	7.699 (67wt%)	0.769	3.07

Table 2. Specifications of samples

Sample	RTV-2	ATH	Silica	Modification ratio (Stearic acid:Silica)
rh	70wt%	30wt%	0	-
rhs1e1	69wt%	30wt%	1wt%	1:1 (se1 nanoparticles)
rhs3e1	67wt%	30wt%	3wt%	1:1 (se1 nanoparticles)
rhs1e2	69wt%	30wt%	1wt%	2:1 (se2 nanoparticles)
rhs3e2	67wt%	30wt%	3wt%	2:1 (se2 nanoparticles)

Characterization

To compare microstructure of the samples, field emission scanning electron microscopy (FE-SEM) was used. FE-SEM images were captured at a magnification of 1000 and a voltage of 15 kV.

The spray test was conducted to determine the hydrophobicity class [18]. The desired surface (preferably an area of 50-100 cm² with a maximum length-to-width ratio of 3 to 1) was sprayed with water, preferably distilled or deionized, from a distance of 20 ± 10 cm. The surface should be sprayed continuously for 10 to 20 s. Then, the pattern, shape, and amount of coverage of the drops on the surface were compared visually with the seven classes defined for hydrophobicity in the references according to the STRI92/1 standard. Surface checking should be carried out up to 10 seconds

after the spray test is completed. The entirely hydrophobic surface is equivalent to HC1 class, and the fully hydrophilic surface is equivalent to HC7. To determine the static contact angle, a water drop with a particular volume is placed on the sample. The drop was imaged by a high-resolution camera, and finally, the software of the contact angle measuring system measures the contact angle using image processing techniques. This test was conducted at several points on the surface for more accurate results. Eventually, the average contact angle was declared.

The hardness test was carried out according to ISO868 (Shore A) standard [27]. The tensile strength test was performed following the ISO37 standard, which is the most common standard for rubbers. The dumbbell-shaped sample was stretched by a Universal Testing Machine at a speed of 10 mm/min This test specifies a method for determining the tensilestress–strain properties of vulcanized and thermoplastic rubbers [28]. Elastic modulus can be calculated from the slope of the tensile test stress/strain graph when the material obeys Hooke's law.

The dielectric constant was determined according to the ISO37 standard. To measure the surface resistance, the test must be performed at 23 °C according to IEC 62631-3-2 standard; the desired voltage was applied, and after 1 min, the surface resistance was measured.

Results and Discussion

Microstructure

Figure 2 is the image of the sample containing 3wt% silica, in which silica nanoparticles were modified with 2:1 ratio of stearic acid:silica (rhs3e2). Figure 3 is the image of the sample containing 3wt% silica in which silica nanoparticles were modified with 1:1 ratio of stearic acid:silica (rhs3e1).

It seems that rhs3e2 has more and larger agglomerates than rhs3e1. A possible explanation for this result might be that the excess amount of stearic acid in rhs3e2 helped the formation of agglomerates and reduced the chance of adsorbing a uniform fatty acid layer on silica.
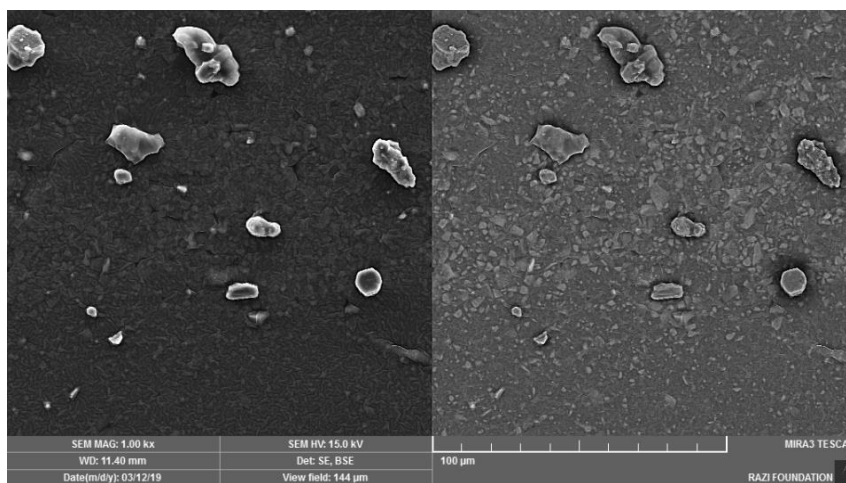

Figure 2. FE-SEM image of rhs3e2 (The sample containing 3wt% silica nanoparticles modified with 2:1 weight ratio of stearic acid:silica)
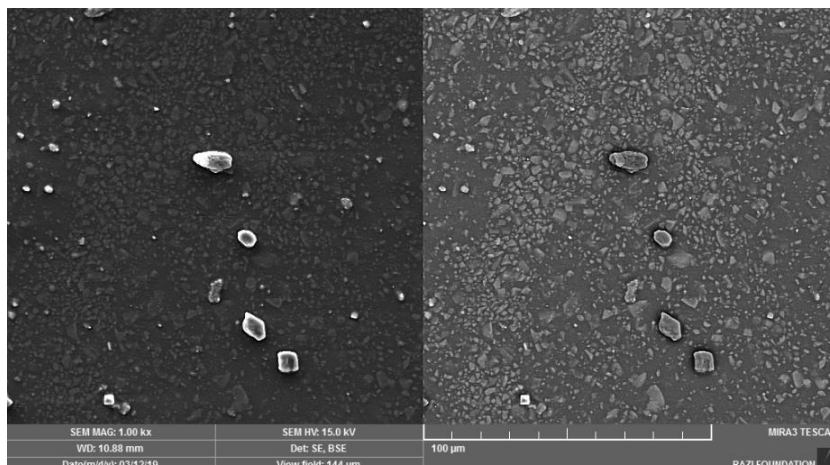
Figure 3. FE-SEM image of rhs3e1 (The sample containing 3wt% silica nanoparticles modified with 1:1 weight ratio of stearic acid:silica)

Hydrophobicity

Due to the natural hydrophilicity of silica nanoparticles, they require surface modification to be uniformly dispersed within the polymer matrix. Without surface modification, the van der Waals intermolecular attraction force between the nanoparticles is so high that the particles tend to agglomerate, this leads to their non-uniform dispersion in the polymer and undermines the polymer properties.

Stearic acid is a type of fatty acid, non-toxic, hydrophobic, non-interacting, inexpensive, and environmentally friendly surface modifier. Carbonyl oxygen of stearic acid molecule can create hydrogen bonds with the silanol hydrogen and cause adsorption of stearic acid onto the silica surface (Fig.4) [1]. The stearic acid molecule has two ends, one hydrophilic and one hydrophobic. Its hydrophilic head is adsorbed to the silica and its hydrophobic tail to the polymer. Thereby it causes bonding between the nanoparticle and the polymer without a chemical reaction [23].
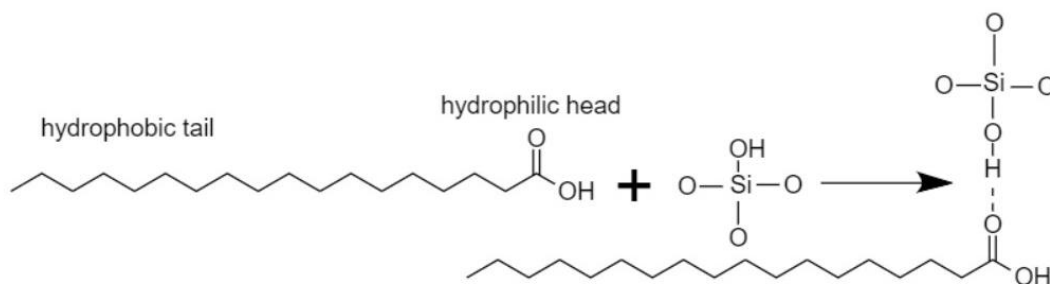

Figure 4. Schematic illustration of physical surface modification of SiO_2 through hydrogen-bond formation between silica and stearic acid molecules [26]

Hydrophobicity class (spray test)

If a surface is hydrophobic, the water drops should be circular when viewed from above,

and hydrophobicity decreases as they depart from the circular shape. Figure 5 reveals some oval-shaped drops on the surface of sample rh, the number of oval-shaped drops decreased

with increasing silica content in the sample, indicating an increase in hydrophobicity [28]. This is due to the surface roughness that silica nanoparticles have created [29]. Based on the comparison of the spray test results with the existing criteria, it seems that the hydrophobicity class of the sample rh is equivalent to HC2 (high and desirable hydrophobicity), and the hydrophobicity class of the samples containing silica is equivalent to HC1, which is an entirely hydrophobic surface.

When a surface has a nanometer-scale roughness, the interface area between air and water on the surface increases, and the capillary force between the water drop and the surface decreases sharply. Therefore, the water drop becomes spherical [29]. Many researchers have shown that hydrophobic surfaces can be achieved by adding low-energy nanoparticles to a suitable polymer matrix [15].
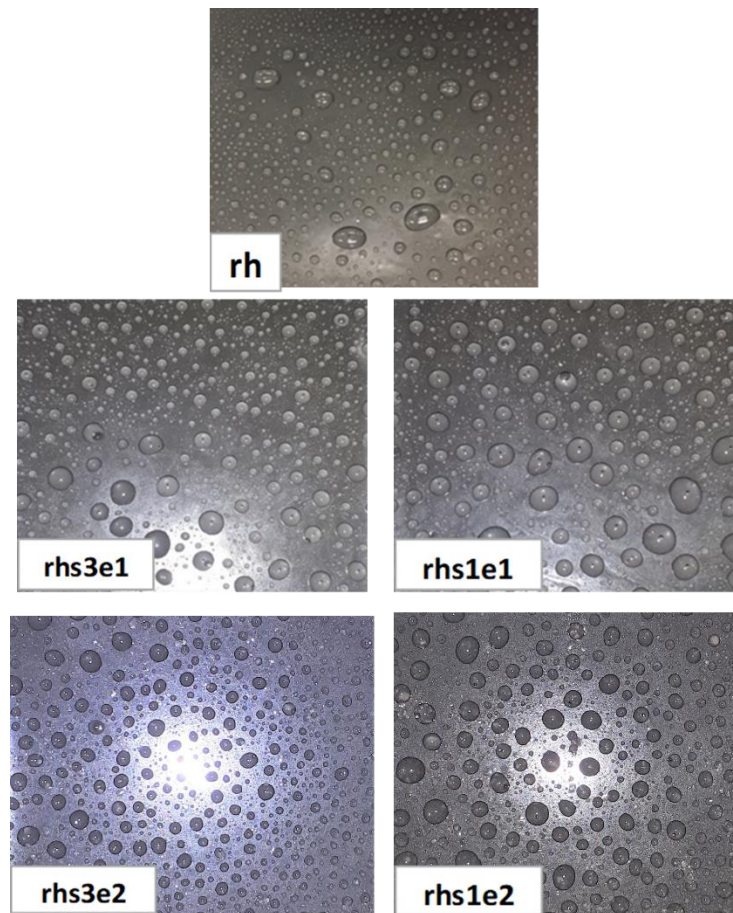

Figure 5. Images of water-sprayed pure and nanocomposite samples indicating hydrophobicity class according to STRI92/1 standard

Contact angle

Figure 6 shows water drops on the samples, and Figure 7 demonstrates the static contact angle test results. It can be seen from Figures 6 and 7 that the nanocomposite samples

containing 1wt% silica have greater contact angles. When the weight percent of nanoparticles increases, the possibility of agglomeration also increases. The contact angle increased from 102 to 112 degrees when 1wt% of silica nanoparticles with a modification ratio

of 1:1 were added. According to Figure 7, the smaller contact angle of composite samples with a higher amount of stearic acid can be attributed to the larger and more agglomerates, which can be observed in Figure 2.
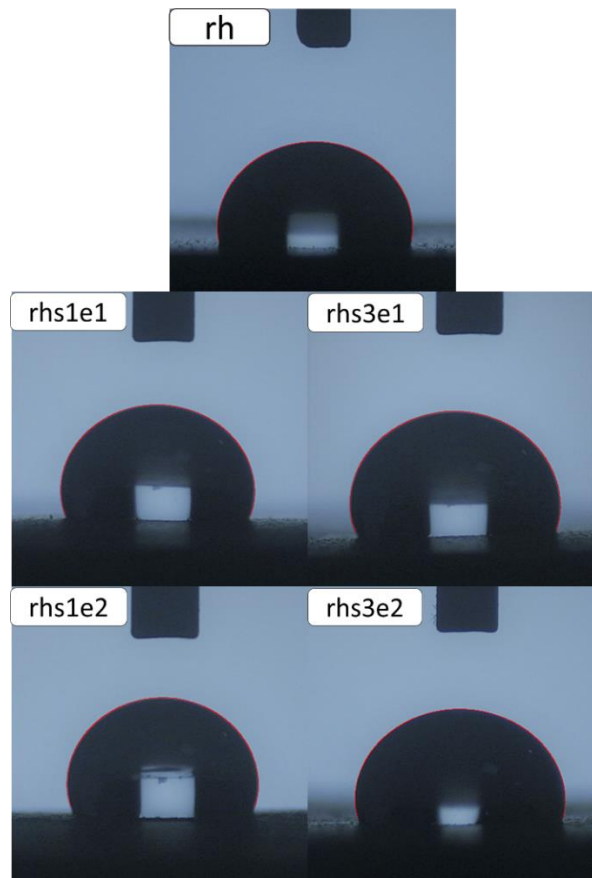

Figure 6. Contact angle images of pure and nanocomposite samples
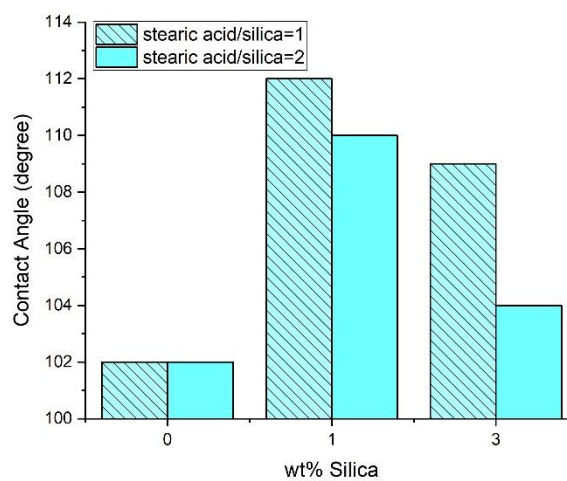

Figure 7. Static contact angles of pure and nanocomposite samples as a function of silica content with different modification ratios

Mechanical properties

Nanoparticles act as physical crosslinkers that restrict the movement of polymer chains and increase tensile modulus and strength [18, 30]. Authors have reported that adding nanoparticles up to an optimum amount can improve the crosslinking of a polymer and thus increase the hardness, while higher filler content may interfere with the crosslinking reaction between the polymer chains [18, 31].

The average hardness of the samples are shown in Figure 8. As it can be seen, the addition of se1 (1:1 ratio of stearic acid: silica) to RTV-2 increased its hardness, but the addition of se2 (2:1 ratio of stearic acid: silica) decreased it. This is due to excess stearic acid in the composite because stearic acid is a fatty acid that softens the sample [23].

It is well-known that the polymer's elastic modulus (tensile modulus) increases when ceramic filler such as silica is incorporated [2, 3, 24, 32]. Figure 8 shows that this happened to the samples of this study, too. The elastic modulus of the samples containing se1 increased with increasing filler content. However, there is a decrease in the elastic modulus of the samples containing se2 with increasing filler content. Another study observed a similar result in composite samples containing higher stearic acid concentration [23]. The decrease in the elastic modulus of the samples containing se2 can be explained by the plasticizing effect of the excess stearic acid that became a multilayer on the surface of filler particles [23]. However, all composite samples have a higher elastic modulus than the pure one.
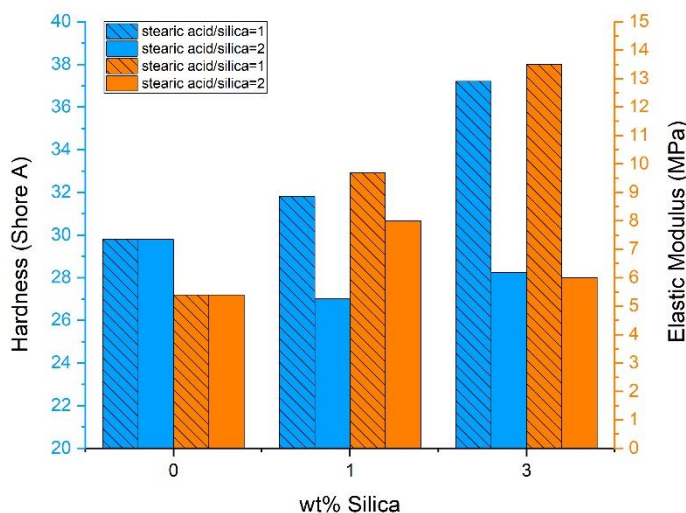

Figure 8. Hardness and elastic modulus of pure and nanocomposite samples as a function of silica content with different modification ratios

Adding filler to the RTV matrix reduces tensile strength; this is common for composites with weak interfacial interactions [33, 34]. In this study, the tensile strengths of the composite samples have decreased. The results are indicated in Table 3 and Figure 9. The tensile strength of a filled polymer is difficult to predict

because it depends strongly on polymer-filler interactions. One problem is the insufficient bonding between filler and polymer, which results in poor stress transfer [2, 23, 35]. Using stearic acid as a modifier, Seon Hoon Ahn *et al*. [23] found that the tensile strength of the silica-reinforced poly(ethylene 2,6-naphthalate)

(PEN) decreased with increasing silica content due to the non-homogeneous dispersion. As the filler percentage increases, agglomeration of the nanoparticles occurs due to the strong interaction between them, leading to failure when an external force is applied [23]. rhs1e2 had lower tensile strength than rhs1e1 due to excess stearic acid in the composite. Researchers have noted that if the surface modification and dispersion of the nanoparticles are correctly done, the mechanical properties of the composite will improve [23, 24, 36]. Authors reported that tensile properties improve with increasing silica concentration up to a specific amount. In contrast, a further increase in the filler content led to a deterioration in some mechanical parameters [24, 37].

The fracture strain of the samples are shown in Figure 9. Normally, the addition of hard ceramic fillers to a polymer matrix decreases the elongation at break (fracture strain) [2, 24]. Still, if there is a good reinforcement between polymer and filler, fracture strain will increase [2]. According to Figure 9, we can see an increase in fracture strain of the samples containing se1, indicating a good reinforcement. However, as the concentration of se2 increases from 1wt% to 3wt%, the fracture strain decreases sharply. It seems that the samples with higher stearic acid concentration had poorer filler adhesion to the polymer matrix [2], which could be predicted from FE-SEM images (Fig.2-3). Figure 10 indicates the stress-strain curves of the samples compared to each other.

Table 3. Values of Tensile properties

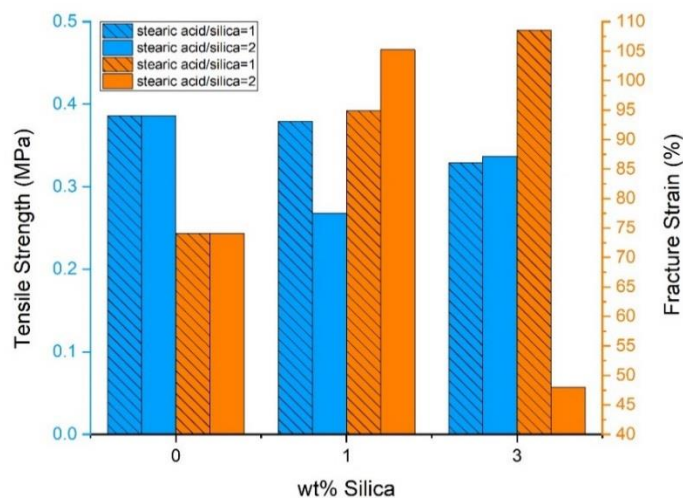| Sample	Force peak(N)	Stress peak(MPa)	Fracture strain (%)	Thickness(mm)
rh	2.130	0.386	74.1	1.38
rhs1e1	2	0.379	94.9	1.32
rhs3e1	1.67	0.329	108.55	1.27
rhs1e2	0.96	0.268	105.25	0.89
rhs3e2	1.59	0.337	48	1.18

Figure 9. Tensile strength and fracture strain of pure and nanocomposite samples as a function of silica content with different modification ratios
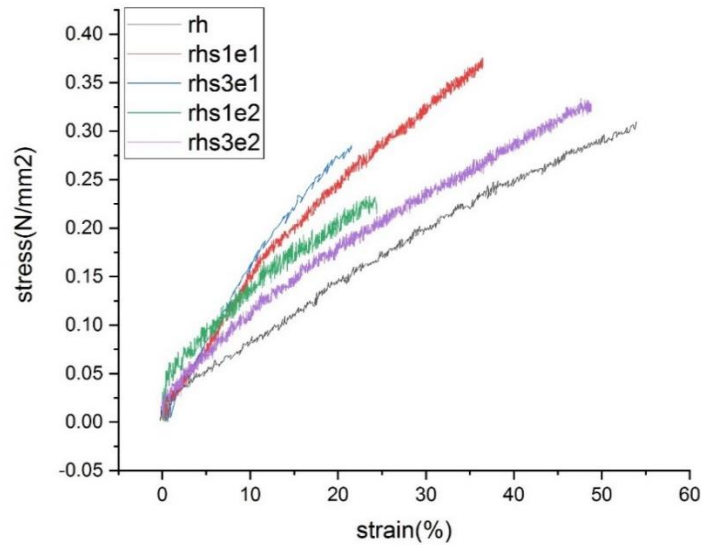
Figure 10. Stress-strain curves of pure and nanocomposite samples

Electrical properties

Dielectric constant & dielectric loss factor

The interface between the polymer and the nanoparticle has a critical role in determining the dielectric properties of a composite [38, 39]. Significant reduction in leakage current and dielectric loss and improvement in dielectric strength occurred when suitable functional groups were located at the polymer-particle interface. Properties of the interfaces between the polymer and the particles, which are nanometric in dimensions, are responsible for improving electrical properties [39]. It was observed that the bare nanoparticle surfaces are inherently relatively conducive. Improvement in the dielectric properties of nanocomposites could be due to the change in polymer morphology at the interface, local charge distributions, and charge mobility [39].

The results of dielectric tests are listed in Table 4 and plotted in Figure 11. Dielectric constant was calculated according to equation 1 where C is capacitance and d is sample thickness.

$$\varepsilon_r = 0.0564 Cd \qquad (1)$$

The dielectric constant of all composite samples is lower than that of the pure sample. Adding high surface-energy ceramic nanoparticles into a low surface-energy polymer creates highly non-homogeneous electric fields at the interfaces that can conduct charge due to improper dispersion [39]. The volume fraction of the polymer surrounding the filler particle is affected by the particle surface and has properties different from the bulk polymer. This area is called the interaction zone [40]. Some authors have emphasized that the interaction zone is a "quasi-conductive" region that partially overlaps in the nanocomposite [40]. This interaction zone is much more extensive for nanocomposites than for micro composites. M. Roy *et al*. [40] observed a decrease in the dielectric constant of the SiO_2-polyethylene nanocomposite to a level lower than the base resin. They concluded that the increase in the interfacial region in nanocomposites creates a zone of altered polymer properties, reducing the dielectric constant of nanocomposites. Tanaka *et al*. [41] demonstrated that adding nano-silica particles

made the conductivity higher compared to microparticles. However, other studies indicate increased dielectric constant with the introduction of silica nanoparticles to a polymer matrix [42, 43].

The dielectric loss factor of all composite samples is lower than that of the pure sample. Lihong Cheng *et al.* [43] also found that the dielectric losses were reduced by adding nano-silica particles to epoxy.

Table 4. Dielectric constant and dielectric loss factor values of pure and nanocomposite samples.

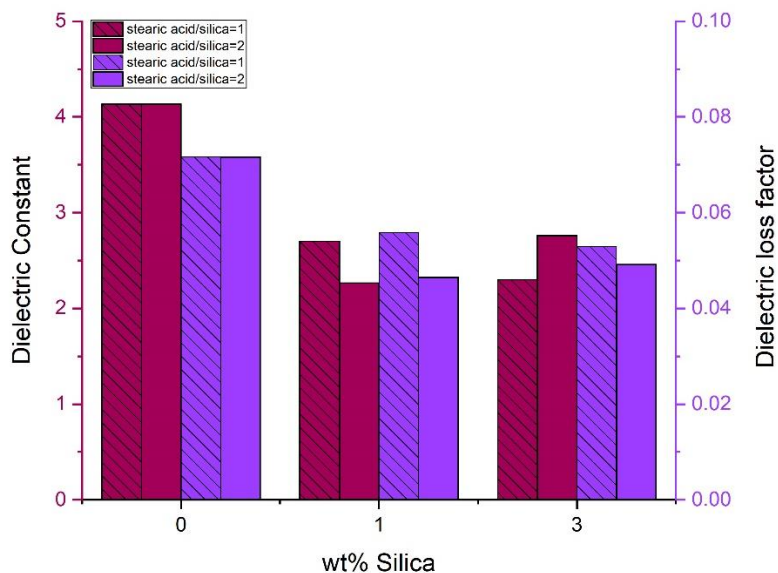| Sample	Dielectric constant(ε_r)	Capacitance (pF)	Dielectric loss factor	Frequency (Hz)	Voltage (V)	Thickness(mm)
rh	4.1343	49.53	7.158×10^{-2}	50	100	1.48
rhs1e1	2.7	36.53	5.588×10^{-2}	50	100	1.32
rhs3e1	2.3	32.5	5.289×10^{-2}	50	100	1.27
rhs1e2	2.265	45.128	4.643×10^{-2}	50	100	0.89
rhs3e2	2.76	41.528	4.916×10^{-2}	50	100	1.18

Figure 11. Dielectric constant and dielectric loss factor of pure and nanocomposite samples as a function of silica content with different modification ratios

Surface resistance

Surface resistance is the insulator's surface resistance to current leakage. Therefore, higher surface resistance will reduce the current leakage [44]. The results of the surface resistance test are indicated in Table 5 and Figure 12. Specific surface resistance was calculated according to equations 2-3 where R_x

is the measured surface resistance, and p is the effective environment of test electrodes.

$$\rho = R_x \frac{p}{g} \tag{2}$$

$$p = \pi(d_1 + g), \ d_1 = 49.5 \times 10^{-3}(m), \ g = 1 \times 10^{-3}(m) \tag{3}$$

The results indicate that the surface resistance increased by adding modified silica to the RTV-2 matrix. Surface resistance

enhancement in all composite samples is attributed to the presence of modified silica nanoparticles [45]. Among all investigated samples, rhs1e2 has the highest measured surface resistance and calculated specific surface resistance. This may be due to the stronger bonds between silicon and oxygen atoms and increased interactions between silica and the polymer matrix [45].

Table 5. Values of Surface resistance

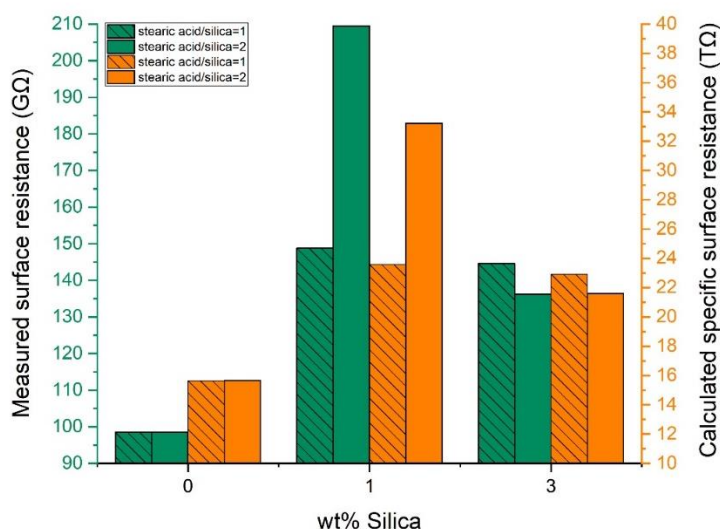| Sample	Calculated specific surface resistance(TΩ)	Measured surface resistance(GΩ)	Voltage (V)	Thickness (mm)
rh	15.66	98.5	1000	1.48
rhs1e1	23.59	148.8	1000	1.32
rhs3e1	22.929	144.6	1000	1.27
rhs1e2	33.22	209.5	1000	0.89
rhs3e2	21.597	136.2	1000	1.18

Figure 12. Measured and calculated specific surface resistance of pure and nanocomposite samples as a function of silica content with different modification ratios

Conclusion

In this research, we used inexpensive and environmentally friendly stearic acid instead of expensive silane coupling agents or hazardous fluorinated hydrocarbons for surface modification of silica nanoparticles. RTV-2/SiO$_2$-free films with different silica loadings (1wt% and 3wt%) modified with different concentrations of stearic acid (stearic acid:silica weight ratio of 1:1 and 2:1) were prepared.

The highest increase in contact angle (10 degrees) was observed in the sample containing 1wt% silica modified with a lower amount of stearic acid. In contrast, a further increase in silica content decreased the contact angle. However, all nanocomposite samples showed a greater contact angle than the pure one.

FE-SEM images and results of the mechanical properties test indicated that the proper surface modification was not done in the samples containing silica modified with a higher amount of stearic acid. This excess amount of stearic acid prevented the adsorption of a uniform layer on the surface of nanoparticles. It led to the larger agglomerates and poor adhesion and dispersion of the filler. Adding silica nanoparticles modified with a lower concentration of stearic acid increased the hardness of RTV-2, while adding silica modified with double the amount of stearic acid reduced the hardness. The sample containing 3%wt silica with the modification ratio of 1:1, had the highest hardness, elongation at break, and tensile modulus compared to the pure and other composite samples.

In summary, in addition to the filler concentration, the modification ratio of nanoparticles plays a crucial role in determining the nanocomposite properties. The addition of silica nanoparticles with a modification ratio of 1:1 improved the hydrophobicity, hardness, tensile modulus, elongation at break, dielectric loss factor, and electrical surface resistance of RTV-2 silicone rubber, while the excess amount of stearic acid had the most adverse effect on the mechanical properties. Therefore it seems that RTV-2/SiO$_2$ nanocomposite coating containing 1wt% stearic acid-modified silica with a modification ratio of 1:1 has the potential for coating the ceramic outdoor insulators in polluted areas.

Disclosure Statement

No potential conflict of interest was reported by the authors.

Acknowledgments

Orcid

Leila Sohrabi-Kashani ⓘ: 0000-0002-2311-2510
Ashkan Zolriasatein ⓘ: 0000-0002-3324-1367
Bijan E. Yekta ⓘ: 0000-0003-2397-8944

References

[1]. Ali S.I., Ali S.R., Naeem M., Haq S.A., Mashhood M., Ali A., Hasan S.A. *J. Basic Appl. Sci.,* 2016, **12**:339 [Google Scholar]

[2]. Abraham R, Thomas S.P., Kuryan S., Isac J., Varughese K.T., Thomas S. *Express Polym. Lett.,* 2009, **3**:177 [Google Scholar]

[3]. Han C., Im H.G., Park H.Y., Yoon S.Y., Kang D.J. *Ceram. Int.,* 2019, **45**:16688 [Crossref], [Google Scholar], [Publisher]

[4]. Nizamuddin S., Maryam S., Baloch H.A., Siddiqui M.T.H., Takkalkar P., Mubarak N.M., Jatoi A.S., Abbasi S.A., Griffin G.J., Qureshi K., Kao N. *Sustainable Polymer Composites and Nanocomposites*, Springer, 2019, p 899 [Crossref], [Google Scholar], [Publisher]

[5]. Wang F., Pi J., Song F., Feng R., Xu C., Wang X.L., Wang Y.Z. *Chem. Eng. J.,* 2020, **381**:122539 [Crossref], [Google Scholar], [Publisher]

[6]. Lv L., Liu H., Zhang W., Chen J. Liu Z. *Mater. Lett.,* 2020, **258**:126653 [Crossref], [Google Scholar], [Publisher]

[7]. Seyedmehdi S.A., Ebrahimi M. *Prog. Org. Coat.,* 2018, **123**:134 [Crossref], [Google Scholar], [Publisher]

[8]. Hejazi I., Hajalizadeh B., Seyfi J., Sadeghi G.M.M., Jafari S.H., Khonakdar H.A., *Appl. Surf. Sci.,* 2014, **293**:116 [Crossref], [Google Scholar], [Publisher]

[9]. Qing Y., Yang C., Hu C., Zheng Y., Liu C. *Appl. Surf. Sci.,* 2015, **326**:48 [Crossref], [Google Scholar], [Publisher]

[10]. Qing Y., Zheng Y., Hu C., Wang Y., He Y., Gong Y., Mo Q. *Appl. Surf. Sci.,* 2013, **285**:583 [Crossref], [Google Scholar], [Publisher]

[11]. Awais M., Jalil M., Zulfiqar U., Husain S.W. *IOP Conference Series: Materials Science and Engineering,* 2016 [Crossref], [Google Scholar], [Publisher]

[12]. Seyedmehdi S.A., Ebrahimi M., *Prog. Org. Coat.,* 2018, **124**:99 [Crossref], [Google Scholar], [Publisher]

[13]. Cao L., Jones A.K., Sikka V.K., Wu J., Gao D. *Langmuir,* 2009, **25**:12444 [Crossref], [Google Scholar], [Publisher]

[14]. Zuo Z., Liao R., Guo C., Zhao X., *2015 IEEE Conference on Electrical Insulation and Dielectric Phenomena (CEIDP),* 2015 [Crossref], [Google Scholar], [Publisher]

[15]. Momen G., Farzaneh M. *Rev. Adv. Mater. Sci,* 2011, **27**:1 [Google Scholar]

[16]. Ullah I., Akbar M., Khan H.A. *Mater. Chem. Phys.,* 2022, **282**:125972 [Crossref], [Google Scholar], [Publisher]

[17]. Zolriasatein A., RajabiMashhadi Z., Abadchi M.R., Noori N.R., Abyazi S. *J. Renew. Energy Environ.,* 2022, **9**:45 [Crossref], [Google Scholar], [Publisher]

[18]. Sohrabi-Kashani L., Yekta B.E., Rezaie H.R., Zolriasatein A. *J. Mater. Sci.: Mater Electron.* 2022,**33**:14488 [Crossref], [Google Scholar], [Publisher]

[19]. Farhang F., Ehsani M., Jazayeri S.H. *Iran. Polym. J.* 2009, **18**:149 [Google Scholar]

[20]. Nazir M.T., Phung B.T., Hoffman M. *2015 IEEE 11th International Conference on the Properties and Applications of Dielectric Materials (ICPADM),* 2015 [Crossref], [Google Scholar], [Publisher]

[21]. Amin M., Khattak A., Ali M. *Electrical Engineering,* 2018, **100**:217 [Crossref], [Google Scholar], [Publisher]

[22]. Meyer L.H., Cabral S.H.L., Araújo E., Cardoso G., Liesenfeld N. *Conference record of the 2006 IEEE international symposium on electrical insulation,* 2006, 474 [Crossref], [Google Scholar], [Publisher]

[23]. Ahn S.H., Kim S.H., Lee S.G. *J. Appl. Polym. Sci.,* 2004, **94**:812 [Crossref], [Google Scholar], [Publisher]

[24]. Lai Y.H., Kuo M.C., Huang J.C., Chen M. *Materials Science and Engineering: A,* 2007, **458**:158 [Crossref], [Google Scholar], [Publisher]

[25]. Deniz S., Arikin B. *Int. J. Eng. Appl. Sci.,* 2016, **8**:19 [Google Scholar]

[26]. Sohrabi-Kashani L, Zolriasatein A., Yekta B.E., *Bull. Mater. Sci.,* 2022, **45**:163 [Crossref], [Google Scholar], [Publisher]

[27]. UNEEN ISO, *868: 2003 Standard. Plastics and Ebonite—Determination of Indentation Hardness by Means of a Durometer (Shore Hardness)(ISO 868: 2003)* [Google Scholar]

[28]. Zolriasatein A., Navazani S., Abadchi M.R., Noori N.R. *J. Mater. Sci: Mater. Electron.,* 2021, **32**:8903 [Crossref], [Google Scholar], [Publisher]

[29]. Simpson J.T., Hunter S.R., Aytug T. *Rep. Prog. Phys.,* 2015, **78**:086501 [Crossref], [Google Scholar], [Publisher]

[30]. Hassanajili S., Sajedi M.T., *Iran. Polym. J.,* 2016, **25**:697 [Crossref], [Google Scholar], [Publisher]

[31]. Abd El-Fattah M., El Saeed A.M., Dardir M.M., El-Sockary M.A. *Prog. Org. Coat.,* 2015, **89**:212 [Crossref], [Google Scholar], [Publisher]

[32]. Liu D., Song L., Song H., Chen J., Tian Q., Chen L., Sun L., Lu A., Huang C., Sun G. *Compos. Sci. Technol.,* 2018, **165**:373 [Crossref], [Google Scholar], [Publisher]

[33]. Du B.X., Xu H. *IEEE Trans. Dielectr. Electr. Insul.,* 2014, **21**:511 [Crossref], [Google Scholar], [Publisher]

[34]. Meyer L.H., Jayaram S.H., Cherney E.A. *IEEE Transactions on Dielectrics and Electrical insulation,* 2005, **12**:1201 [Crossref], [Google Scholar], [Publisher]

[35]. Nair A.B., Vijayan D., Ayswarya E.P., Joseph R., Nah, C. *J. Adv. Nanomater.,* 2017, **2**:83 [Crossref], [Google Scholar], [Publisher]

[36]. Khan H., Amin M., Ahmad A., Yasin M. *Journal of Elastomers & Plastics,* 2018, **50**: 501 [Crossref], [Google Scholar], [Publisher]

[37]. Chiulan I., Panaitescu D.M., Radu E.R., Frone A.N., Gabor R.A., Nicolae C.A., Jinescu G., Tofan V., Chinga-Carrasco G. *J. Mech. Behav. Biomed. Mater.,* 2020, **101**:103427 [Crossref], [Google Scholar], [Publisher]

[38]. Aradhya R., Renukappa N.M., *Improved Dielectric Properties of Epoxy Nano Composites*, In *Optimum Composite Structures*, IntechOpen, 2018 [Google Scholar]

[39]. Siddabattuni S., Schuman T.P., Dogan F. *ACS Appl. Mater. Interfaces,* 2013, **5**:1917 [Crossref], [Google Scholar], [Publisher]

[40]. Roy M., Nelson J.K., MacCrone R.K., Schadler L.S., Reed C.W., Keefe R., *IEEE transactions on dielectrics and electrical insulation,* 2005, **12**:629 [Crossref], [Google Scholar], [Publisher]

[41]. Tanaka T., *IEEE Trans. Dielectr. Electr. Insul.,* 2005, **12**:914 [Crossref], [Google Scholar], [Publisher]

[42]. Veena M.G., Renukappa N.M., Shivakumar K.N., Seetharamu S. *Sādhanā,* 2016, **41**:407 [Crossref], [Google Scholar], [Publisher]

[43]. Cheng L., Zheng L., Li G., Yao Z., Yin Q., Jiang K. *Int. J. Nanoparticles,* 2008, **1**:3 [Google Scholar]

[44]. Zolriasatein A., Mashhadi Z.R., Navazani S., Abadchi M.R., Noori N.R., Abdi N. *J. Mater. Sci.: Mater. Electron.,* 2021, **32**:12265 [Crossref], [Google Scholar], [Publisher]

[45]. Khan H., Amin M., Ali M., Iqbal M., Yasin M. *Turk. J. Elec. Eng. Comp. Sci.,* 2017, **25**:1426 [Crossref], [Google Scholar], [Publisher]